

RESEARCH ARTICLE | FEBRUARY 22 1998

Molecular scale precursor of the liquid–liquid phase transition of water

Eli Shiratani; Masaki Sasai



J. Chem. Phys. 108, 3264–3276 (1998)

<https://doi.org/10.1063/1.475723>



View
Online



Export
Citation

CrossMark

Articles You May Be Interested In

Quantifying the destructuring of a thixotropic colloidal suspension using falling ball viscometry

Physics of Fluids (January 2021)

Molecular interpretation of water structuring and destructuring effects: Hydration of alkanediols

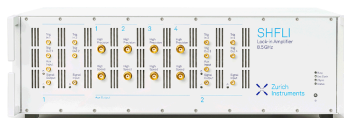
J. Chem. Phys. (December 2004)

Growth and collapse of structural patterns in the hydrogen bond network in liquid water

J. Chem. Phys. (May 1996)

500 kHz or 8.5 GHz?
And all the ranges in between.

Lock-in Amplifiers for your periodic signal measurements



Find out more



Molecular scale precursor of the liquid–liquid phase transition of water

Eli Shiratani and Masaki Sasai

Graduate School of Human Informatics, Nagoya University, Nagoya 464-01, Japan

(Received 2 September 1997; accepted 21 November 1997)

Spatiotemporal fluctuations of the local structure in liquid water are studied with the molecular-dynamics simulation. At temperatures around and above the melting point, each molecule alternately goes through the structured period and the destructured period. Lifetime of each period spreads from several hundred fs to 10 ps at 0 °C at 1 atm. The order parameter to describe this structural switching fluctuations is derived by carefully filtering out the fast oscillating components from the simulation data. By analyzing the neutron-weighted pair correlation function, we find that the clusters of the structured molecules and the clusters of the destructured molecules are similar to the clusters of low-density amorphous (LDA) ice and the clusters of high-density amorphous (HDA) ice, respectively. Simulated liquid water is, therefore, a composite of the LDA-like clusters and the HDA-like clusters even at temperatures well above the melting point. The large amplitude structural fluctuation of water at around and above the melting temperature should be regarded as the molecular-scale precursor of the possible liquid–liquid phase transition in the supercooled region.

© 1998 American Institute of Physics. [S0021-9606(98)51408-0]

I. INTRODUCTION

A most striking feature of liquid water is that fluctuations in entropy and density become anomalously large when liquid water is supercooled below the melting temperature.¹ The origin and mechanism of this anomaly, however, have not yet been elucidated.^{2,3} Mishima *et al.*^{4,5} showed that there exists the first-order transition between high-density amorphous (HDA) ice and low-density amorphous (LDA) ice. As shown in Fig. 1, it is natural to assume that the experimentally observed transition lines between HDA-ice and LDA-ice can be extrapolated to the transition lines between high-density liquid (HDL) and low-density liquid (LDL). Then, it should be plausible to consider that this hypothetical HDL–LDL transition is responsible for the anomalously large thermodynamic fluctuations.^{6–10} Recent molecular-dynamics (MD) simulations suggested that the HDL–LDL transition lines are terminated by the critical point located in the supercooled region^{7–9} or in the negative-pressure region.¹⁰ The large fluctuation around the critical point might be the origin of the thermodynamic anomaly of supercooled liquid water.^{7–10}

If this hypothetical critical point of the HDL–LDL transition exists, then in the higher temperature region than the critical point, the fluctuations should be observed as growth and collapse of “droplets” or “micro-domains” of two different liquid states. In other words, the fluctuations should be described in terms of the clusters of the HDA-like molecules or the clusters of the LDA-like molecules. Indeed, there are evidences that liquid water is a mixture of two different states of molecules over the wide range of temperature.^{11–15} For example, isosbestic points were observed by superposing Raman spectra of different temperatures both in the low frequency intermolecule-vibration band¹¹ and in the high frequency intramolecule-vibration band.¹² Existence of the isosbestic points suggests that the Raman spectrum is a

superposition of signals from two different states.¹² The Voronoi analysis of the MD data suggested that there are two different states of molecules with different geometrical arrangement of neighboring molecules.¹³ The MD simulation of the hydrogen-bond network revealed that the molecules with four hydrogen bonds distribute inhomogeneously in space and form the clusters of the four-bonded molecules.^{14,15} Thus, it is important to understand the relation between the possible liquid–liquid transition in the supercooled region and the MD and experimental evidences for the spatially inhomogeneous fluctuations in the higher temperature region. The characteristic of the molecular-scale fluctuations over the wide temperature region needs to be understood so as to reveal the consistent view of the macroscopic anomaly of supercooled water.

In order to examine whether the characteristic of the fluctuations is described in terms of the clusters of two different liquid states, it is important to find a suitable order parameter which can distinguish the difference in the local structure of liquid water. Therefore, it is a key issue to define the order parameter by extracting the slow and fundamental change of the structural pattern from the rapidly oscillating noisy data of the MD simulation.

Since the radial distribution is most fundamental information of the liquid state, the radial distribution function around the individual molecules should be a useful probe to study the spatiotemporal variation of the local structure. By using the MD simulation with the TIP4P potential,¹⁶ Shiratani and Sasai¹⁷ examined the temporal variation of the radial distribution function around the arbitrarily chosen central molecule and showed that each molecule alternately went through two different periods; the structured period during which the local hydrogen-bond structure is more developed than the average, and the destructured period during which the local hydrogen-bond structure is less developed. The lifetime of these periods spreads from several hundred fs

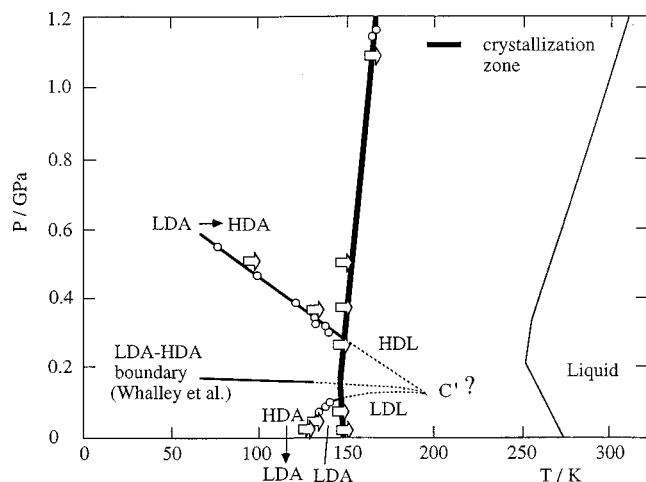


FIG. 1. Schematic phase diagram of water. The thin real lines are the line melting from ices to liquid, the line of transition from HDA-ice to LDA-ice, the line of transition from LDA-ice to HDA-ice, and the line of coexistence of HDA-ice and LDA-ice. The location of the line of coexistence of HDA-ice and LDA-ice was suggested by Whalley *et al.* (Ref. 26). The thick lines are crystallization from HDA-ice or from LDA-ice. White circles are the experimental data of transition induced by changing pressure, and white arrows are the experimental data of transition induced by changing temperature: These data were taken from Ref. 5. The dashed lines are the transition lines between HDL and LDL obtained by extrapolating the transition lines between HDA-ice and LDA-ice. C' is the hypothetical critical point of the liquid-liquid transition, whose position was suggested to be in the supercooled region (Refs. 7 and 8) or in the negative-pressure region (Ref. 10). Liquid water around the melting temperature could have the large fluctuations associated with the possible HDL-LDL transition.

(1 fs = 10^{-15} s) to a few ps (1 ps = 10^{-12} s) at 25 °C at 1 atm. In order to quantify this structural fluctuation, a new index, local structure index (LSI) was introduced.¹⁷ LSI is a second moment of the radial distribution function, which efficiently characterizes the shape of the function. In the destructured period, LSI of the water molecule is kept small and such molecule was termed the destructured molecule. In the structured period, on the other hand, LSI of the molecule is rapidly oscillating with large amplitude. Such molecule was termed the structured molecule.

Shiratani and Sasai showed that the structured molecules tend to be close to each other to form clusters.¹⁷ However, the originally defined LSI in Ref. 17 was a rapidly oscillating function of time due to the fast librational and translational motions of molecules. Owing to these oscillations, the definition of the cluster was rather obscured. It was not conclusive, therefore, whether there was a significant tendency that clusters of the structured molecules were formed. In the present paper, the fast oscillating components of LSI are carefully filtered out with a new technique of coarse-graining and the coarse-grained LSI (C-LSI) is used as an order parameter to describe the local structural fluctuation. Structured and destructured molecules are re-defined in terms of C-LSI. Through the examination of the neutron-weighted pair correlation function, $h(r)$, it is shown that the structured molecule is LDA-like and the destructured molecule is HDA-like. There are clear tendencies of the LDA-like clusters and the HDA-like clusters to be formed, so that the fluctuations of liquid water above the melting temperature are described

by the growth and collapse of the LDA-like clusters and the HDA-like clusters.

It should be also interesting to examine the relation between LSI and other local physical quantities, such as the potential energy, the local number of surrounding molecules, the local number of hydrogen bonds, and the local number of rings in the hydrogen-bond network. Through comparisons with these local indices, the physical meaning of LSI is clarified.

The present paper is organized as follows: In Sec. II the MD simulations are explained. In Sec. III LSI and C-LSI are discussed. By using C-LSI, it is shown that the structured molecule is LDA-like and the destructured molecule is HDA-like. In Sec. IV the clusters of LDA-like molecules and the clusters of HDA-like molecules are discussed. In Sec. V LSI is compared with other local quantities. The last section is devoted to summary and discussion. The definition of C-LSI is given in the Appendix.

II. MOLECULAR DYNAMICS SIMULATION

MD simulations were performed under the condition of constant volume and constant energy. Both the compressed system under the high pressure and the system at the ambient pressure were examined. In the compressed system, density was fixed at 1.1 g/cm³ and temperature was varied as -21 °C, 4 °C, 27 °C, and 72 °C. In the system at the ambient pressure, density was calibrated in the same way as in Ref. 17 to be the experimental value at 1 atm; -10 °C (0.998 25 g/cm³), 0 °C (0.999 84 g/cm³), 7 °C (0.999 90 g/cm³), 25 °C (0.997 074 g/cm³), and 72 °C (0.976 62 g/cm³). The effect of this density tuning is not so significant and the results should be almost the same as in the system with the constant density at around 0.998 g/cm³. 216 water molecules are confined in a cubic box with the periodic boundary condition. TIP4P potential was used and the long-range interactions were cutoff at the half of the box length. The simulation time step was chosen to be 0.4 fs. The length of the equilibration was set to 22 500 steps in the system at the ambient pressure, and 125 000 steps in the compressed system. After the equilibration, configurations at every 10 fs were sampled to calculate the statistical data. The averages were taken over the trajectory for 100 ps in the ambient pressure system and for 50 ps in the compressed system.

III. ORDER PARAMETER OF THE STRUCTURAL FLUCTUATION

The local oxygen-oxygen radial distribution function $g_{O-O}(r; \mu, t)$ around the molecule μ at time t is defined as

$$g_{O-O}(r; \mu, t) = \frac{\Delta n(r; \mu, t)}{4\pi\rho r^2 \Delta r}, \quad (1)$$

where ρ is the average density, $\rho = N/V$, r is distance from molecule μ , Δr is the range of distance for sampling $\Delta r = 0.05$ Å, and $\Delta n(r; \mu, t)$ is the number of molecules whose O-O distance from the molecule μ is in the range between $r - \Delta r/2$ and $r + \Delta r/2$. Figure 2(a) illustrates the temporal variation of $g_{O-O}(r; \mu, t)$ around the arbitrarily chosen mol-

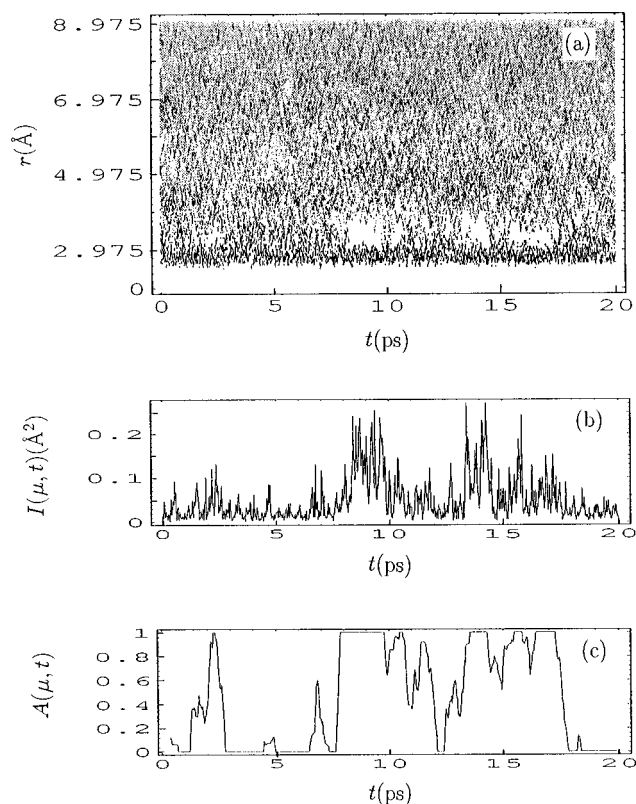


FIG. 2. Temporal variation of the local structure around the arbitrarily chosen molecule μ at $T=25$ °C under the ambient pressure. (a) The temporal variation of the local radial distribution function $g_{o-o}(r; \mu, t)$ is shown with the gray-scaled tones. The larger the value of $g_{o-o}(r; \mu, t)$, the darker the tone is. The temporal variation of (b) the local structure index $I(\mu, t)$, and (c) the coarse-grained local structure index $A(\mu, t)$. $A(\mu, t)$ is used as the order parameter which describes the structural switching fluctuations. Definition of $A(\mu, t)$ is given in the Appendix.

molecule μ with the gray-scaled tones. The most remarkable feature of Fig. 2(a) is that there are relatively white regions ranging from $r=3.2$ Å to $r=3.8$ Å for the period from $t=1$ to 2.5 ps, from $t=7$ to 11 ps, and from $t=13$ to 18 ps. In these periods, the tetrahedral structure is locally developed around the centered molecule and the molecules which disturb the local structure have small chance to intervene between $r=3.2$ Å and $r=3.8$ Å. Thus, we call these periods the structured periods. For the period from $t=0$ to 1 ps, from $t=2.5$ to 7 ps, from $t=11$ to 13 ps, and from $t=18$ to 20 ps, on the other hand, the region between $r=3.2$ Å and $r=3.8$ Å is occupied by many lines of moving molecules. During these periods, the open tetrahedral structure is less developed. We call these periods the destructured periods. The centered molecule alternately goes through structured and destructured periods. Distribution of lifetime of these periods hierarchically spreads from several hundred fs to a few ten ps at 0 °C at 1 atm.

In order to quantify this structural switching phenomenon, we define the local structure index (LSI). The oxygen–oxygen distance between the i th molecule and the centered molecule is written as r_i and molecules are numbered in order of distance from the center molecule; $r_1 < r_2 < \dots < r_i < r_{i+1} < \dots < r_{n(\mu, t)} < r_{n(\mu, t)+1}$. $n(\mu, t)$ is chosen so that

$r_{n(\mu, t)} < 3.7$ Å $< r_{n(\mu, t)+1}$. Then LSI, $I(\mu, t)$, of the molecule μ at time t is

$$I(\mu, t) = \frac{1}{n(\mu, t)} \sum_{i=1}^{n(\mu, t)} [\Delta(i; \mu, t) - \bar{\Delta}(\mu, t)]^2, \quad (2)$$

where $\Delta(i; \mu, t) = r_{i+1} - r_i$ and $\bar{\Delta}(\mu, t)$ is the average of $\Delta(i; \mu, t)$

$$\bar{\Delta}(\mu, t) = \frac{1}{n(\mu, t)} \sum_{i=1}^{n(\mu, t)} \Delta(i; \mu, t). \quad (3)$$

Thus, $I(\mu, t)$ expresses inhomogeneity in the radial distribution within the sphere $r < 3.7$ – 3.8 Å. During the structured period, molecules are excluded from the region 3.2 Å $< r < 3.8$ Å, which results in the large value of $I(\mu, t)$.

Figure 2(b) shows that $I(\mu, t)$ is indeed a good measure to distinguish the structured and destructured periods: In the destructured period $I(\mu, t)$ mostly has the value smaller than 0.04 Å², and in the structured period $I(\mu, t)$ is strongly oscillating and often surpasses 0.04 Å². The rapidly oscillating component of LSI is, however, due to the thermal librational and translational vibrations. These vibrations are motions within the fixed hydrogen-bond network structure or at most motions with the small change of the hydrogen-bonding pattern: The rapidly oscillating component of LSI is not directly relevant to the structural switching phenomenon associated with the large-scale network rearrangement. Therefore, it is rather inconvenient to use $I(\mu, t)$ for the statistical analysis: We may be able to define the time duration of $I(\mu, t) > 0.04$ Å², for example, as the structured instance. Such structured instance does not last long due to the oscillation and its lifetime is typically a few hundred fs, much shorter than the lifetime of the structured period. The LSI oscillation of the neighbor molecule is often out of phase, so that the spatial correlation of the structured molecules is underestimated with such definition of the structured state. The simple and naive way to erase the rapid oscillation of $I(\mu, t)$ is to average $I(\mu, t)$ over the time duration of some width. With such averaging, however, information of the fast structural changing is thrown out. To prevent such information loss, a more elaborated method based on the physical ingredient of LSI is needed.

We developed a new method of coarse-graining based on the maximum likelihood estimation.¹⁸ Detailed explanation of this coarse-graining technique is given in the Appendix. The newly defined index is termed the coarse-grained LSI (C-LSI), $A(\mu, t)$, of the molecule μ at time t . In Fig. 2 $A(\mu, t)$ is compared with $g_{o-o}(r; \mu, t)$ and $I(\mu, t)$. The fluctuation of the local structure can be described as a switching motion between the structured state of $A(\mu, t) \approx 1$ and the destructured state of $A(\mu, t) \approx 0$. Thus, $A(\mu, t)$ should be used as the order parameter of the structural fluctuation.

Armed with this new definition of the order parameter, we can discuss many aspects of the structural fluctuation. It was shown^{7,19} that the neutron-weighted pair correlation function $h(r)$ is calculated from the oxygen–oxygen, oxygen–hydrogen, and hydrogen–hydrogen radial distribution functions as

$$h(r) = 4\pi\rho r(0.092g_{\text{O-O}}(r) + 0.422g_{\text{O-H}}(r) + 0.486g_{\text{H-H}}(r) - 1). \quad (4)$$

We extend this definition to the local pair correlation function $h(r; \mu, t)$ around the molecule μ at time t

$$h(r; \mu, t) = 4\pi\rho r(0.092g_{\text{O-O}}(r; \mu, t) + 0.422g_{\text{O-H}}(r; \mu, t) + 0.486g_{\text{H-H}}(r; \mu, t) - 1), \quad (5)$$

where $g_{\text{O-O}}(r; \mu, t)$ is defined by Eq. (1) and $g_{\text{O-H}}(r; \mu, t)$ and $g_{\text{H-H}}(r; \mu, t)$ are defined in the same way for the oxygen–hydrogen and hydrogen–hydrogen radial distribution. Then, $h(r; \mu, t)$ is averaged separately depending on the state of the central molecule μ . Here we define $\theta(\mu, t)$ to distinguish whether the molecule μ at time t is destructured or structured

$$\theta(\mu, t) = \begin{cases} 1 & \text{for } A(\mu, t) > A_{\text{threshold}} \\ 0 & \text{for } A(\mu, t) \leq A_{\text{threshold}} \end{cases}. \quad (6)$$

Here, we use $A_{\text{threshold}} = 0.5$. The motivation of this choice comes from that the distribution functions of lifetime of the structured and destructured periods have the smoothest functional forms with this choice of $A_{\text{threshold}}$ (data not shown). It should be noted, however, that the quantitative results depend sensitively on the value of $A_{\text{threshold}}$. When dependences of the results on $A_{\text{threshold}}$ would be crucial, one has to go back to the original definition of the order parameter $A(\mu, t)$.

$h(r; \mu, t)$ averaged over the structured molecules is denoted by $h_s(r)$

$$h_s(r) = \left\langle \frac{1}{N_s} \sum_{\mu} h(r; \mu, t) \theta(\mu, t) \right\rangle, \quad (7)$$

where N_s is the number of the structured molecules with $\theta = 1$ in the whole system at time t and $\langle \dots \rangle$ is the average over the MD trajectory. $h(r; \mu, t)$ averaged over the destructured molecules is denoted by $h_d(r)$

$$h_d(r) = \left\langle \frac{1}{N_d} \sum_{\mu} h(r; \mu, t) (1 - \theta(\mu, t)) \right\rangle, \quad (8)$$

where N_d is the number of the destructured molecules with $\theta = 0$, $N_s + N_d = N = 216$. In Fig. 3 $h_s(r)$ and $h_d(r)$ thus obtained are compared with the experimental data of $h(r)$ in LDA-ice and $h(r)$ in HDA-ice.²⁰ As schematically shown in Fig. 4, the similarity between $h_s(r)$ and $h(r)$ in LDA-ice and the similarity between $h_d(r)$ and $h(r)$ in HDA-ice are consistent with the picture that liquid water consists of the clusters of the LDA-like molecules and the clusters of the HDA-like molecules even at temperature well above the melting point.

In this section the order parameter of the structure fluctuation $A(\mu, t)$ was introduced, which can effectively describe the structural switching phenomenon of the hydrogen-bond network. By using this order parameter, it was shown that the fluctuations in liquid water at temperature above the melting point should be related to the HDA–LDA transition in a fundamental way. In the next section this relation is

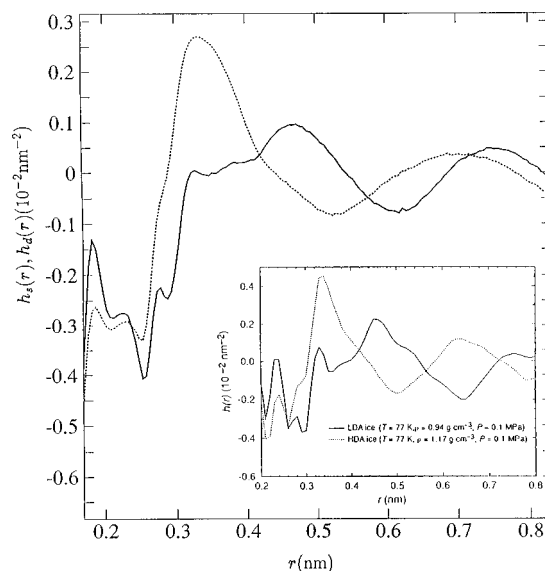


FIG. 3. The neutron-weighted pair correlation function averaged around the structured molecule $h_s(r)$ (real line) and the neutron-weighted pair correlation function averaged around the destructured molecule $h_d(r)$ (dotted line), which are obtained from the MD data at $T = 25^\circ\text{C}$ under the ambient pressure. Inset is the experimentally observed neutron-weighted pair correlation functions $h(r)$ in LDA-ice (real line) and $h(r)$ in HDA-ice (dotted line), which are taken from Ref. 20.

more precisely discussed by examining the clusters of the LDA-like molecules and the clusters of the HDA-like molecules.

IV. LDA-LIKE CLUSTERS AND HDA-LIKE CLUSTERS

In Ref. 17 it was shown that the structured molecules tended to be close to each other to form clusters. In Ref. 17, however, the clusters were defined by the fast oscillating

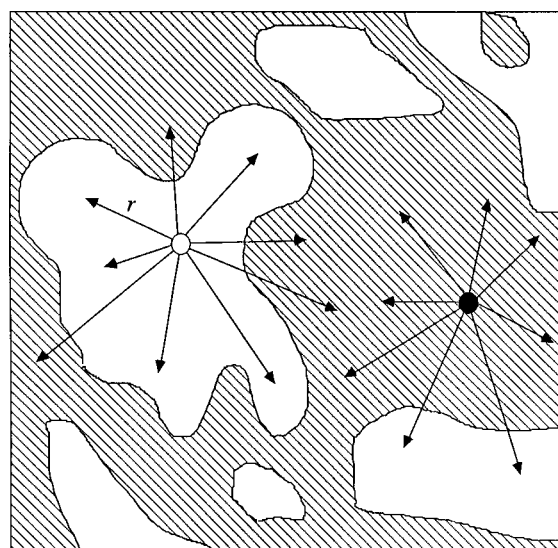


FIG. 4. Schematic representation of the idea that liquid water is a composite of the LDA-like regions (white regions) and the HDA-like regions (hatched regions). Data shown in Fig. 3 are consistent with the picture that $h_s(r)$ is the pair correlation function obtained by looking around from the molecule in the white area and $h_d(r)$ is the pair correlation function obtained by looking around from the molecule in the hatched area.

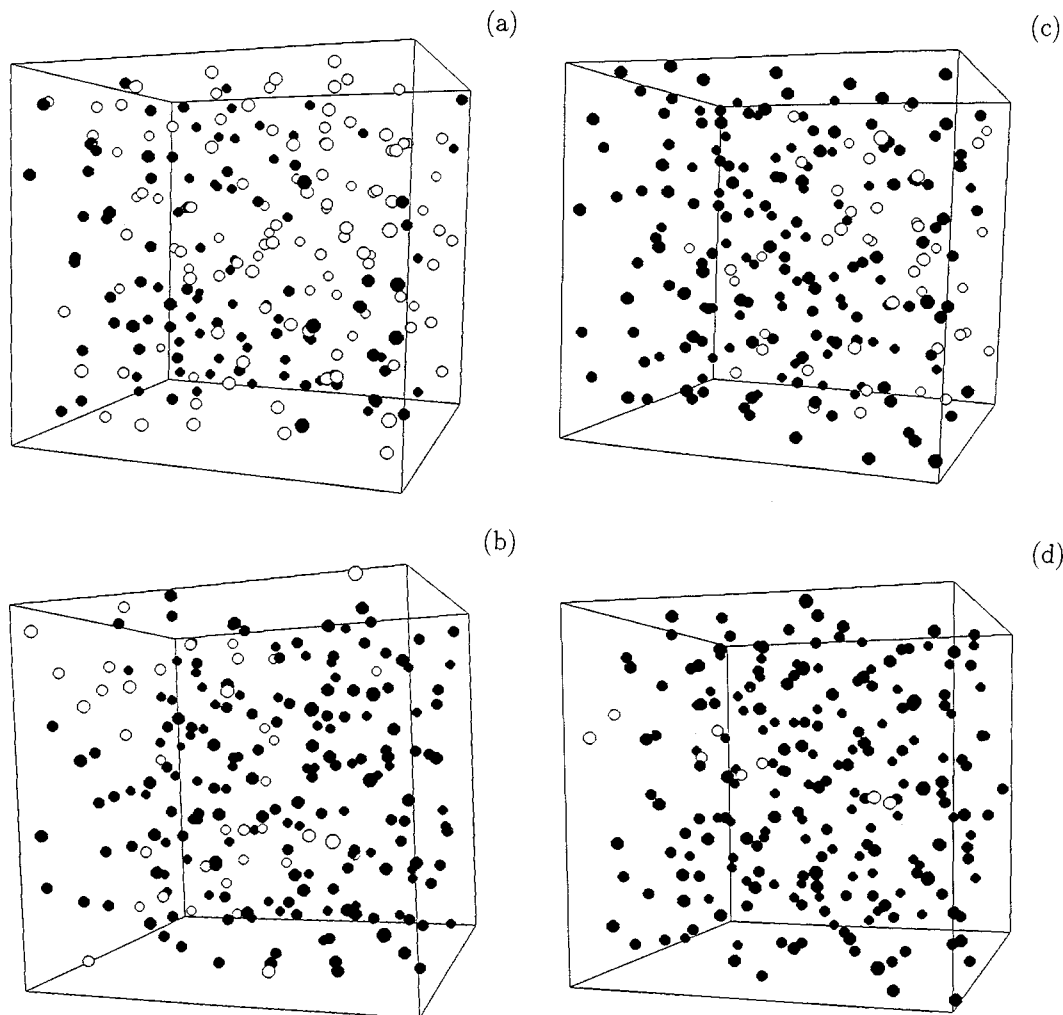


FIG. 5. Snapshots of the MD simulation. The oxygen nuclei of the destructured molecules $A(\mu, t) \leq 0.5$ are shown with filled circles and the oxygen nuclei of the structured molecules $A(\mu, t) > 0.5$ are shown with white circles. (a) $T = -10$ °C under the ambient pressure, (b) $T = 72$ °C under the ambient pressure, (c) $T = -21$ °C in the compressed system, and (d) $T = 72$ °C in the compressed system.

function $I(\mu, t)$, so that the tendency to form clusters was obscured by the large configuration-to-configuration fluctuations. In this section the clusters of the structured and destructured molecules are examined in detail in terms of the new order parameter $A(\mu, t)$ and clear evidences for the correlations to form clusters are shown.

Figures 5(a)–5(d) are snapshots of the MD simulations. Figures 5(a) and 5(b) represent the configurations of molecules at the ambient pressure showing that there exists the region where the structured molecules populate more densely than in other regions. The number of the structured molecules increases as temperature is lowered and the size of the region which is populated densely by the structured molecules increases. Figures 5(c) and 5(d) represent the configurations of molecules in the compressed system. At high temperature of Fig. 5(d) there are small number of the structured molecules scattered in the bulk of the destructured molecules. At the lower temperature of Fig. 5(c), however, there seems to be a tendency that the structured molecules form the cluster.

These impressions received from the MD snapshots are confirmed by examining the correlation between the struc-

tured or destructured molecules. The radial correlation function between the structured molecules is

$$g^s(r) = \left\langle \frac{1}{4\pi r^2 \Delta r \rho_s} \frac{1}{N_s} \sum_{\alpha} \sum_{\beta} \theta(\alpha, t) \times \theta(\beta, t) \Delta(r - r_{\alpha\beta}) \right\rangle, \quad (9)$$

where $\Delta(r - r_{\alpha\beta}) = 1$ when the oxygen–oxygen distance between the molecules α and β is within the range $r - \Delta r/2 \leq r_{\alpha\beta} < r + \Delta r/2$ and $\Delta(r - r_{\alpha\beta}) = 0$ otherwise, and ρ_s is the density of the structured molecules, $\rho_s = N_s/V$. In the same way, the radial correlation function between the destructured molecules is

$$g^d(r) = \left\langle \frac{1}{4\pi r^2 \Delta r \rho_d} \frac{1}{N_d} \sum_{\alpha} \sum_{\beta} (1 - \theta(\alpha, t)) \times (1 - \theta(\beta, t)) \Delta(r - r_{\alpha\beta}) \right\rangle, \quad (10)$$

where ρ_d is the density of the destructured molecules, $\rho_d = N_d/V$.

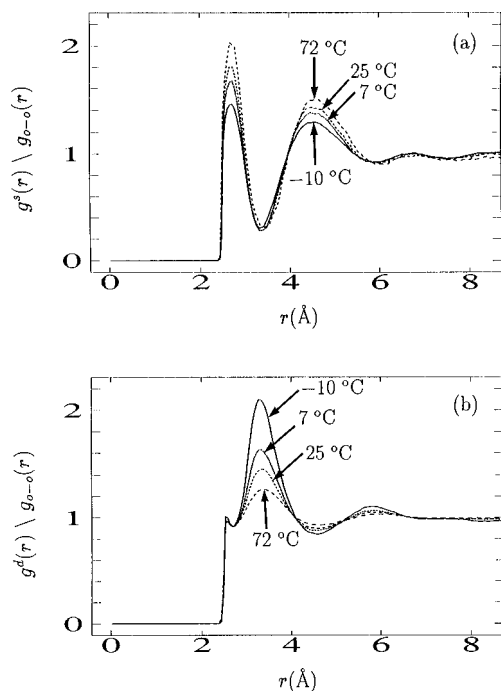


FIG. 6. (a) The radial correlation function between the structured molecules $g^s(r)$ and (b) the radial correlation function between the destructured molecules $g^d(r)$ are shown by normalizing them with the radial distribution function $g_{O-O}(r)$. Calculated from the MD data under the ambient pressure.

In Fig. 6 $g^s(r)$ and $g^d(r)$ are shown by normalizing them with the radial distribution function $g_{O-O}(r)$. As shown in Fig. 6(a), $g^s(r)/g_{O-O}(r)$ is much larger than one for $r < 3.3 \text{ \AA}$. $g^s(r) \gg g_{O-O}(r)$ implies that there is a strong tendency of clusters to be formed. $g^s(r)/g_{O-O}(r)$ has oscillating feature for $r < 7 \text{ \AA}$, which suggests that the structural ordering and the size distribution of clusters extend to the fairly large length scale. The correlation of the structured molecules are weakened as temperature is lowered. This behavior is natural because N_s/N should tend to be one, so that $g^s(r)$ has to resemble to $g_{O-O}(r)$ in the low enough temperature.

As shown in Fig. 6(b), $g^d(r)/g_{O-O}(r) \approx 1$ for $r < 3.3 \text{ \AA}$ and $g^d(r)/g_{O-O}(r) \gg 1$ for $3.3 \text{ \AA} < r < 4 \text{ \AA}$. The correlation between the destructured molecules is largest at somewhat separate distance but the tendency of cluster forming is evident: Figure 6(b) can be explained by assuming the existence of the clusters of the destructured molecules, where each molecule has 2 or 3 destructured neighbors for $r < 3.3 \text{ \AA}$ and 3 or 4 other destructured neighbors at $3.3 \text{ \AA} < r < 4 \text{ \AA}$.

Temperature dependence of the cluster forming tendency is examined by counting the cluster size distribution. We define that the molecule α and the molecule β belong to the same cluster of the structured molecules when the oxygen-oxygen distance between α and β is small, $r_{\alpha\beta} \leq 3.3 \text{ \AA}$ and $\theta(\alpha, t) = 1$ and $\theta(\beta, t) = 1$. In the same way we define that the molecules α and β belong to the same cluster of the destructured molecules when $r_{\alpha\beta} \leq 3.3 \text{ \AA}$, $\theta(\alpha, t) = 0$, and $\theta(\beta, t) = 0$. The probability $P(m_s)$ that the arbitrarily chosen structured molecule belongs to the cluster of size m_s and the probability $P(m_d)$ that the arbitrarily chosen destructured molecule belongs to the cluster of size m_d are

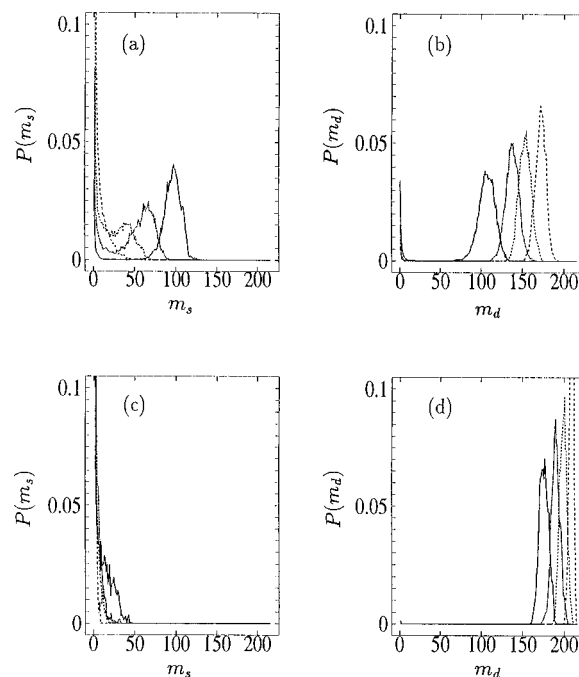


FIG. 7. The probability $P(m_s)$ that the arbitrarily chosen structured molecule belongs to the cluster of size m_s and the probability $P(m_d)$ that the arbitrarily chosen destructured molecule belongs to the cluster of size m_d are shown at various temperatures. (a) $P(m_s)$ and (b) $P(m_d)$ under the ambient pressure at $-10 \text{ }^\circ\text{C}$ (real line), $7 \text{ }^\circ\text{C}$ (dotted line), $25 \text{ }^\circ\text{C}$ (short dashed line), and $72 \text{ }^\circ\text{C}$ (long dashed line). (c) $P(m_s)$ and (d) $P(m_d)$ in the compressed system at $-21 \text{ }^\circ\text{C}$ (real line), $4 \text{ }^\circ\text{C}$ (dotted line), $27 \text{ }^\circ\text{C}$ (short dashed line), and $72 \text{ }^\circ\text{C}$ (long dashed line).

$$P(m_s) = \langle m_s N(m_s, t) / N_s \rangle$$

and

$$P(m_d) = \langle m_d N(m_d, t) / N_d \rangle, \quad (11)$$

respectively. Here $N(m_s, t)$ is the number of the clusters of the structured molecules with size m_s at time t , $N(m_d, t)$ is the number of the clusters of the destructured molecules with size m_d at time t , and $N_s = \sum_{m_s=1}^N m_s N(m_s, t)$ and $N_d = \sum_{m_d=1}^N m_d N(m_d, t)$. Above the melting temperature $N_d > N_s$, so that the system as a whole is dominated by the destructured molecules.

$P(m_s)$ and $P(m_d)$ under the ambient pressure are shown in Fig. 7(a) and in Fig. 7(b). For all the temperatures examined, the system is occupied by a large cluster of the destructured molecules with the size $m_d > 100 \approx N/2$. For the temperatures $T < 25 \text{ }^\circ\text{C}$, however, there appears a large cluster of the structured molecules with the size $m_s < 100 \approx N/2$. In other words, the system is percolated by the structured molecules for $T < 25 \text{ }^\circ\text{C}$, though the system is dominated by the destructured molecules for $T > -10 \text{ }^\circ\text{C}$. Here, too much emphasis should not be laid on the temperature that the structured molecules begin to percolate through the system: The size of the clusters of the structured molecules depend on the threshold $A_{\text{threshold}}$ used to define the cluster. If the severer criterion $A_{\text{threshold}} \approx 1$ is used to define the structured molecules, the cluster size becomes smaller and the temperature of the percolation is lower than $-10 \text{ }^\circ\text{C}$. In the supercooled

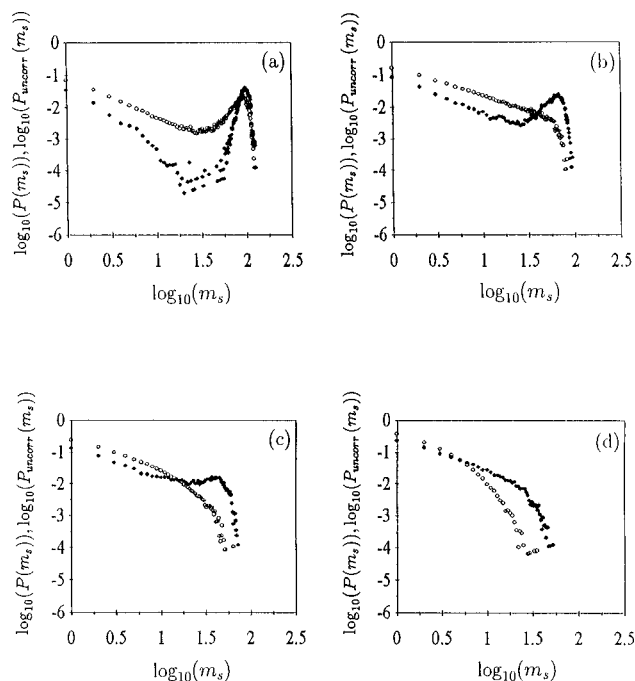


FIG. 8. The probability $P(m_s)$ that the arbitrarily chosen structured molecule belongs to the cluster of size m_s , obtained from the MD data under the ambient pressure is compared with the probability $P_{\text{uncorr}}(m_s)$ calculated under the virtual situation that each molecule is randomly assigned to be in the structured state with the probability N_s/N . $P(m_s)$ is shown with filled circles and $P_{\text{uncorr}}(m_s)$ with white circles. (a) -10°C , (b) 7°C , (c) 25°C , and (d) 72°C .

region below $T \approx -10^\circ\text{C}$, clusters of molecules $A(\mu, t) \leq 0.5$ and clusters of molecules $A(\mu, t) > 0.5$ have almost the same distribution, which implies that the structural fluctuations become so large that the system is not decided whether it should be destructured or structured as a whole.

In the compressed system, as shown in Figs. 7(c) and 7(d), the destructured molecules are predominant in the system. The clusters of the structured molecules do not percolate through the system at all the temperatures examined. Thus in the compressed system, fluctuations associated with growth and collapse of the clusters should be much smaller than in the ambient pressure system.

In Figs. 8 and 9 $P(m_s)$ and $P(m_d)$ under the ambient pressure are shown with the log-log scale. Also shown are the distribution functions $P_{\text{uncorr}}(m_s)$ and $P_{\text{uncorr}}(m_d)$ of the size m_s and m_d of the clusters of the uncorrelated molecules which are calculated under the virtual situation that each molecule is either in the structured or destructured state with the probability N_s/N or N_d/N independently of other molecules. Figure 8 shows that $P(m_s) < P_{\text{uncorr}}(m_s)$ for small m_s and $P(m_s) > P_{\text{uncorr}}(m_s)$ for large m_s for all the temperatures examined. These data imply that the structured molecules in the MD results have a clear tendency to be close to each other comparing to the case that the same number of the structured molecules are randomly distributed in the system without correlation.

As shown in Fig. 9, difference between $P(m_d)$ and $P_{\text{uncorr}}(m_d)$ is much smaller than difference between $P(m_s)$ and $P_{\text{uncorr}}(m_s)$. Correlations among destructured molecules become significant only in the supercooled region at around

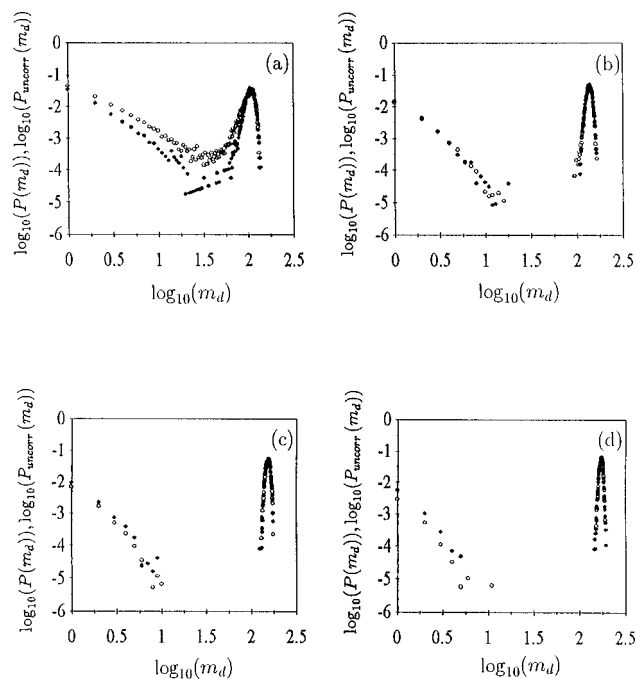


FIG. 9. The probability $P(m_d)$ that the arbitrarily chosen destructured molecule belongs to the cluster of size m_d , obtained from the MD data under the ambient pressure is compared with the probability $P_{\text{uncorr}}(m_d)$ calculated under the virtual situation that each molecule is randomly assigned to be in the destructured state with the probability N_d/N . $P(m_d)$ is shown with filled circles and $P_{\text{uncorr}}(m_d)$ with white circles. (a) -10°C , (b) 7°C , (c) 25°C , and (d) 72°C .

-10°C . It should be interesting to examine whether the correlation among the destructured molecules grows large to the same extent as the correlation among the structured molecules at the low enough temperature.

The structured molecules have a tendency to form clusters and the residual regions of the system should be regarded as the clusters of the destructured molecules. Comparing these results with the results shown in Fig. 3, it is reasonable to identify the clusters of the structured molecules and the clusters of the destructured molecules defined here as the LDA-like clusters and the HDA-like clusters, respectively. Liquid water above the melting temperature is HDA-like as a whole but the motions of the LDA-like clusters embedded within it should decisively affect the characteristic of the fluctuations.

Under the ambient pressure, by lowering temperature, the representative size of the LDA-like clusters become larger and the molecules in the HDA-like clusters begin to spatially correlate to each other. By extrapolating this tendency to the lower temperature region, it is plausible to expect that the statistical properties of the LDA-like clusters and the HDA-like clusters become similar to each other. The fluctuations between the two molecular states should be largest in such circumstance, which can be regarded as a sign that the observed system is in the vicinity of the critical point. Existence of the LDA-like clusters and the HDA-like clusters at the temperature above the melting point is consistent with the hypothesis of the HDL-LDL transition. Thus, it is possible to regard the large fluctuation above the melting temperature as the molecular-scale precursor of the liquid-

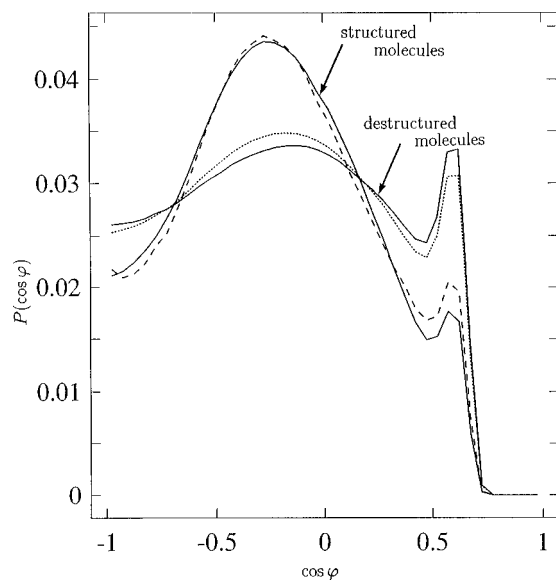


FIG. 10. The angular distribution functions $P(\cos \varphi)$ around the structured molecules and around the destructured molecules are compared with the angular distribution functions around the four-bonded molecules (dashed line) and around the molecules whose number of the hydrogen bonds is other than four (dotted line). $T=25^\circ\text{C}$ under the ambient pressure.

liquid phase transition. Further systematic investigation at the lower temperature region should provide insight into the nature and structure of the thermodynamic anomaly of liquid water.

V. LSI AND OTHER LOCAL INDICES

Since LSI is defined by the local radial distribution of molecules, it is necessary to examine the correlation between LSI and the local angular distribution of molecules. Taking a pair of molecules, α and β for example, whose oxygen–oxygen distances are $r \leq 3.5 \text{ \AA}$ from the centered molecule μ at time t , the angle φ is defined by connecting oxygen nuclei by the line as $\alpha\text{-}\mu\text{-}\beta$. As shown in Fig. 10, the distribution function of $\cos \varphi$ is separately sampled depending on whether the central molecule is structured $\theta(\mu, t) = 1$ or destructured $\theta(\mu, t) = 0$.

For the destructured case, the distribution function $P(\cos \varphi)$ has a broad peak at $\varphi \approx 95^\circ$ and the sharp peak at $\varphi \approx 54^\circ$. The sharp peak at $\varphi \approx 54^\circ$ is the characteristic feature of the five coordinated molecules.²¹ For the structured case, on the other hand, $P(\cos \varphi)$ has a peak at $\varphi \approx 105^\circ$, which is the feature of the tetrahedral ordering of the neighbor molecules. Also shown in Fig. 10 are $P(\cos \varphi)$ for the case that the central molecule μ has four hydrogen bonds and $P(\cos \varphi)$ for the case that the number of the hydrogen bonds of the central molecule is other than four. Similarity between $P(\cos \varphi)$ for the four-bonded molecule and $P(\cos \varphi)$ for the destructured molecule is consistent with the picture that the structured molecule has a tetrahedral ordering around it. The structured molecule, therefore, is expected to have the lower potential energy due to the energy stabilization by the tetrahedral hydrogen-bond forming. The destructured molecule, on the other hand, is expected to have the higher potential energy and should have the larger local den-

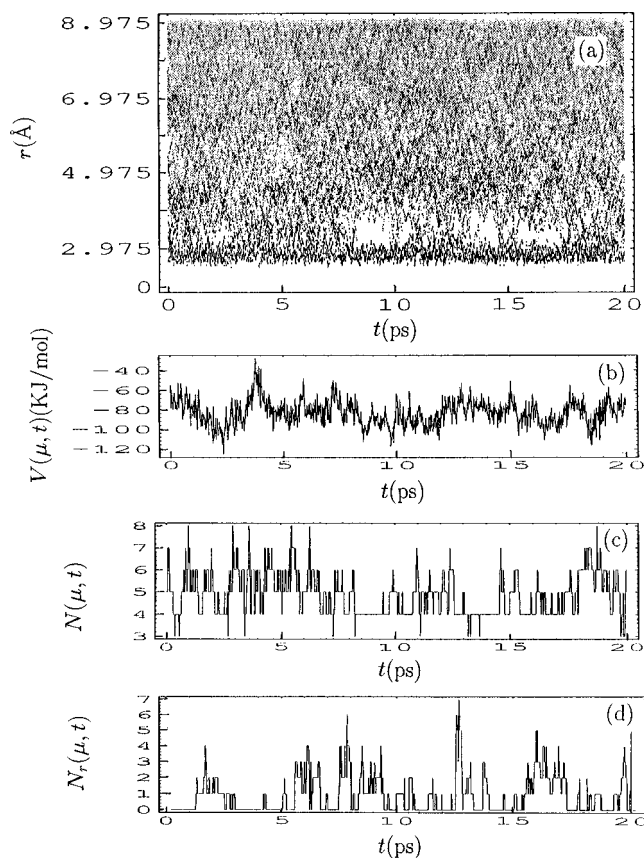


FIG. 11. (a) Temporal variation of the local radial distribution function $g_{0-0}(r; \mu, t)$ is compared with the temporal variation of (b) the potential energy $V(\mu, t)$, (c) the local number of the neighboring molecules $N(\mu, t)$, and (d) the local number of rings in the hydrogen-bond network $N_r(\mu, t)$. Temporal variation of $g_{0-0}(r; \mu, t)$ is the same as Fig. 2(a).

sity of neighbor molecules owing to the tendency to be five or more coordinated. It should be important, then, to examine how well the variation of LSI coincides with the variation of other local quantities such as the potential energy, the local density of molecules and the local number of hydrogen bonds. It is also interesting to see the relation between LSI and the index of the intermediate length scale such as the number of rings in the hydrogen bond network.

We define $V(\mu, t)$ as the potential energy of the molecule μ at time t , $N(\mu, t)$ as the number of molecules whose oxygen–oxygen distance is $r \leq 3.5 \text{ \AA}$ from the centered molecule μ at time t , $N_{\text{HB}}(\mu, t)$ as the number of hydrogen bonds of the molecule μ at time t , and $N_r(\mu, t)$ as the number of rings in the hydrogen bond network, where the molecule μ is involved in the rings as a constituent at time t . Here the hydrogen bond is defined as the relation between two molecules whose interaction energy averaged over 600 fs is less than -15 kJ/mol . We also define $\bar{V}(\mu, t)$ and $\bar{N}(\mu, t)$ as the average of $V(\mu, t)$ and $N(\mu, t)$ over 600 fs.

In Fig. 11, $V(\mu, t)$, $N(\mu, t)$, and $N_r(\mu, t)$ are compared with $g_{0-0}(r; \mu, t)$. From $g_{0-0}(r; \mu, t)$, we can see that roughly speaking the molecule μ is in the structured period from $t=1\text{--}2.5 \text{ ps}$, from $t=7\text{--}11 \text{ ps}$, and from $t=13\text{--}18 \text{ ps}$. Indeed, $V(\mu, t)$ is low from $t=1\text{--}2.5 \text{ ps}$ and from $t=7\text{--}11 \text{ ps}$, but is high from $t=13\text{--}18 \text{ ps}$. $V(\mu, t)$ is

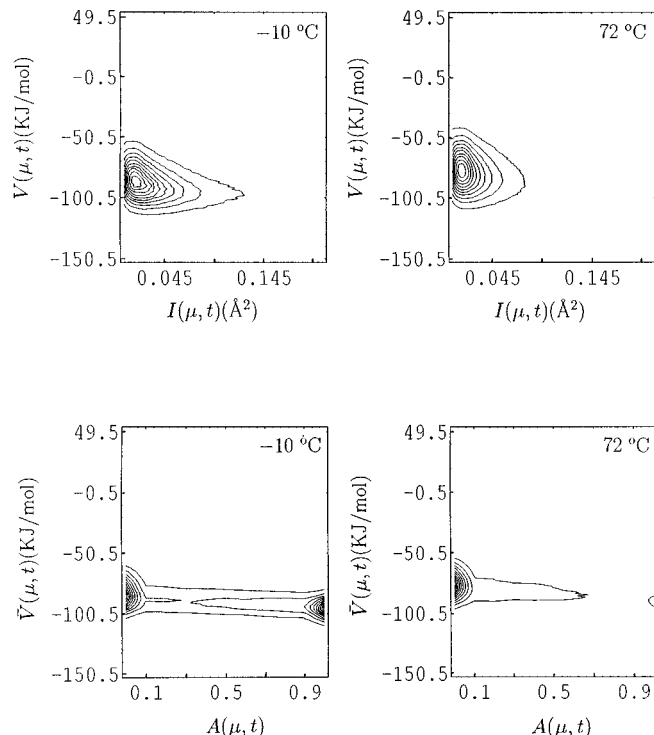


FIG. 12. Contour plots of the correlation $P(I,V)$ between LSI $I(\mu,t)$ and the potential energy $V(\mu,t)$ at -10°C and 72°C , and the correlation $P(A,\bar{V})$ between C-LSI $A(\mu,t)$ and the potential energy averaged over 600 fs $\bar{V}(\mu,t)$ at -10°C and 72°C . The system is under the ambient pressure.

low, on the other hand, during the destructured period from $t=18\text{--}20$ ps. Thus, there is only an imperfect correspondence between the potential energy and the structural switching phenomenon observed with $g_{\text{O-O}}(r;\mu,t)$. Same is true for $N(\mu,t)$, and $N_r(\mu,t)$.

The correlation between LSI and $V(\mu,t)$, $N(\mu,t)$, $N_{\text{HB}}(\mu,t)$, or $N_r(\mu,t)$ is graphically depicted in Figs. 12–15 by defining the two body distribution functions

$$P(I,X) = \langle p(I,X,t) \rangle \quad \text{and} \quad P(A,Y) = \langle p(A,Y,t) \rangle, \quad (12)$$

where $p(I,X,t)$ is the fraction of molecules which have the LSI value I and the other local index X at the same time t . X is $V(\mu,t)$, $N(\mu,t)$, $N_{\text{HB}}(\mu,t)$, or $N_r(\mu,t)$. $p(A,Y,t)$ is the fraction of molecules whose C-LSI value is A and the value of the other local index is Y at time t . Y is $\bar{V}(\mu,t)$, $\bar{N}(\mu,t)$, $N_{\text{HB}}(\mu,t)$, or $N_r(\mu,t)$.

From Figs. 12–15 negative correlation is found between $I(\mu,t)$ and $V(\mu,t)$ and between $I(\mu,t)$ and $N(\mu,t)$ and positive correlation is found between $I(\mu,t)$ and $N_{\text{HB}}(\mu,t)$ and between $I(\mu,t)$ and $N_r(\mu,t)$. $P(I,X)$, however, appears as a rather broad anisotropic peak, which implies that the correlations are not so much significant.

$P(A,Y)$ shows an interesting feature: At -10°C , $P(A,Y)$ consists of two major peaks at $A(\mu,t) \approx 0$ and $A(\mu,t) \approx 1$. Splitting of $P(A,Y)$ into two peaks reflects the two-state nature of the switching fluctuation, that is, $A(\mu,t)$ does not spend much time at the transient region of $A(\mu,t) \approx 0.5$. At 72°C the peak height at the structured state becomes much lower than the peak at the destructured state.

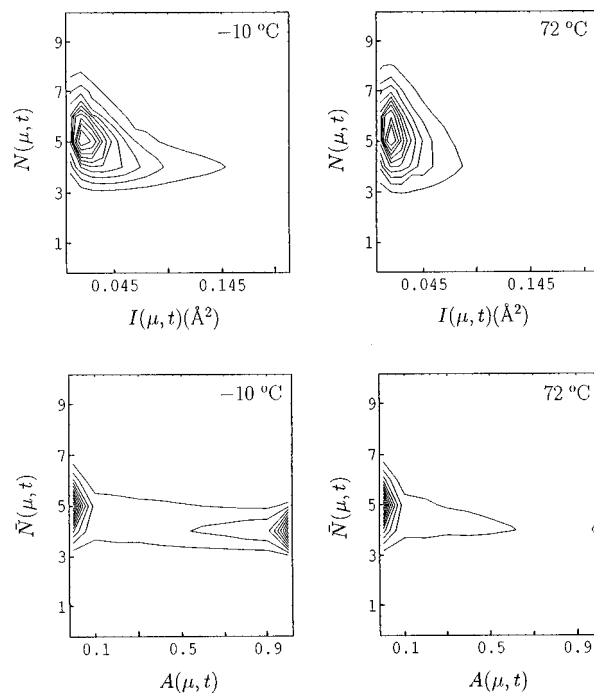


FIG. 13. Contour plots of the correlation $P(I,N)$ between LSI $I(\mu,t)$ and the local number of the neighboring molecules $N(\mu,t)$ at -10°C and 72°C , and the correlation $P(A,\bar{N})$ between C-LSI $A(\mu,t)$ and the local number of the neighboring molecules averaged over 600 fs $\bar{N}(\mu,t)$ at -10°C and 72°C . $\bar{N}(\mu,t)$ takes real value but $N(\mu,t)$ takes only the integer values. Contour plots of $P(I,N)$ are drawn by interpolation. The system is under the ambient pressure.

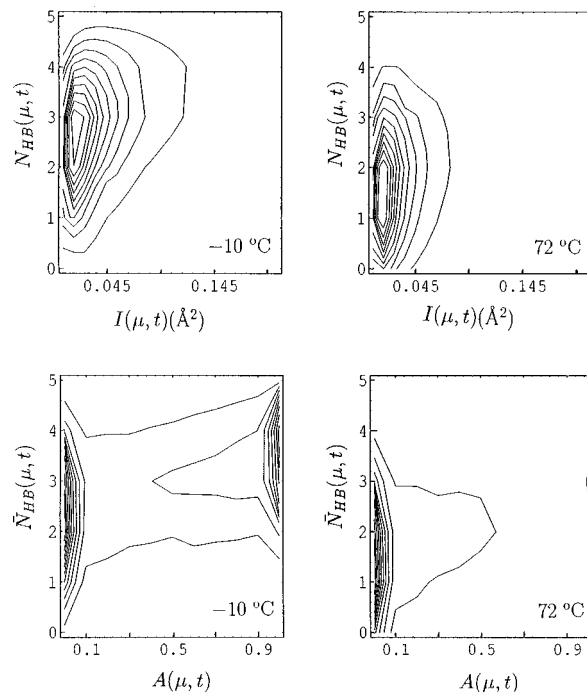


FIG. 14. Contour plots of the correlation $P(I,N_{\text{HB}})$ between LSI $I(\mu,t)$ and the local number of hydrogen bonds $N_{\text{HB}}(\mu,t)$ at -10°C and 72°C , and the correlation $P(A,N_{\text{HB}})$ between C-LSI $A(\mu,t)$ and $N_{\text{HB}}(\mu,t)$ at -10°C and 72°C . Though $N_{\text{HB}}(\mu,t)$ has only the integer values, contour plots are drawn by interpolating $P(I,N_{\text{HB}})$. The system is under the ambient pressure.

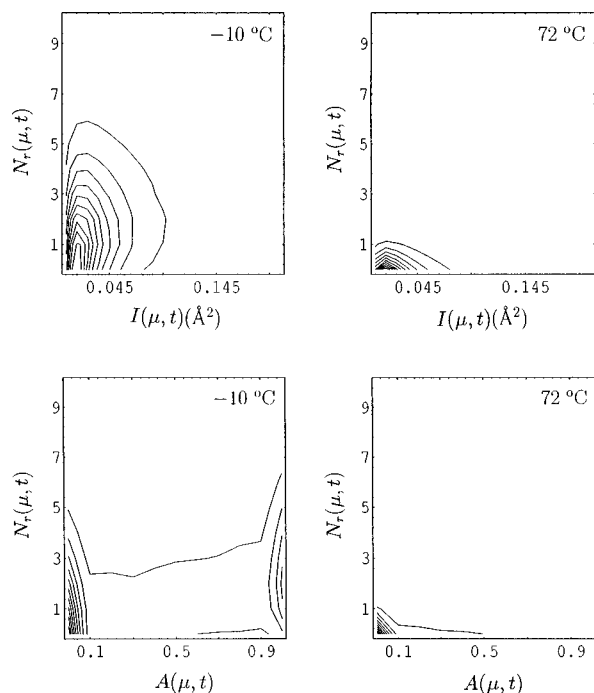


FIG. 15. Contour plots of the correlation $P(I, N_r)$ between LSI $I(\mu, t)$ and the local number of rings in the hydrogen-bond network $N_r(\mu, t)$ at $-10\text{ }^\circ\text{C}$ and $72\text{ }^\circ\text{C}$, and the correlation $P(A, N_r)$ between C-LSI $A(\mu, t)$ and $N_r(\mu, t)$ at $-10\text{ }^\circ\text{C}$ and $72\text{ }^\circ\text{C}$. Though $N_r(\mu, t)$ has only the integer values, contour plots are drawn by interpolating $P(I, N_r)$ and $P(A, N_r)$. The system is under the ambient pressure.

The feature of $P(A, Y)$ splitting into the two peaks, however, is still retained, which suggests that the fluctuations have the switching-type nature even at $72\text{ }^\circ\text{C}$. For all the temperatures examined, positions of two peaks shift from each other in the consistent direction with the positive or negative correlation between LSI and Y : The structured molecules have lower potential energy, smaller number of neighboring molecules, and are involved in the larger number of hydrogen-bond rings than the destructured molecules. However, the amount of the shift of two peaks is not large enough to characterize the structural state of each molecule: $\bar{V}(\mu, t)$, $\bar{N}(\mu, t)$, $N_h(\mu, t)$, or $N_r(\mu, t)$ is not a good measure to distinguish the structured and destructured states in a concise way. For example, $4 < \bar{N}(\mu, t) < 6$ in the destructured state and $3 < \bar{N}(\mu, t) < 5$ in the structured state, so that it is rather difficult to classify the structural state of the molecule μ with $4 < \bar{N}(\mu, t) < 5$. Weak correlations of these local quantities to C-LSI are consistent with the imperfect correspondences between the local quantities and the structure switching phenomenon shown in Fig. 11.

Correlations are larger in the ambient pressure system than in the compressed system and become stronger as temperature is lowered. This temperature-pressure dependences of correlations are quantitatively shown in Fig. 16 by using the mutual information H .

$$H = \left\langle \sum_I \sum_X p(I, X, t) \log \frac{p(I, X, t)}{p(I, t) p(X, t)} \right\rangle, \quad (13)$$

where $p(I, t) = \sum_X p(I, X, t)$ and $p(X, t) = \sum_I p(I, X, t)$. At the very low temperature such as the temperature below the ex-

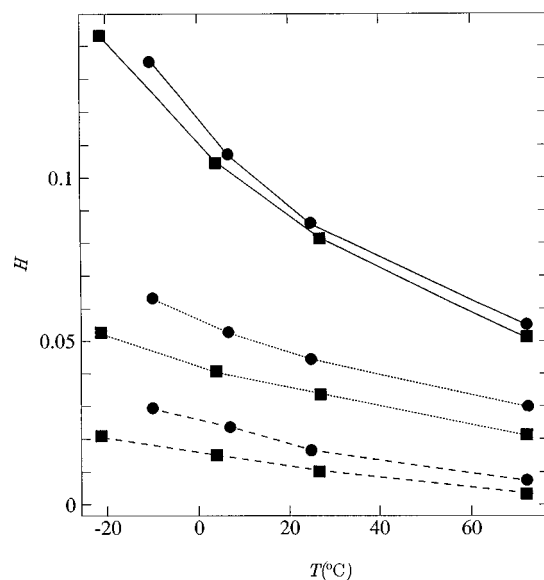


FIG. 16. Temperature dependence of the correlation between LSI and other local quantities are shown in terms of the mutual information. Mutual information between LSI and the potential energy (real line), between LSI and the local number of neighboring molecules (dotted line), and between LSI and the local number of rings in the hydrogen-bond network (dashed line) for the ambient pressure system (●) and for the compressed system (■).

pected critical point, we could find that the other indices also become good order parameters to distinguish the structural state of the individual molecule.⁹ At higher temperatures, on the other hand, the structural switching phenomenon is smeared out by the thermal oscillations and the distinction between the LDA-like molecules and HDA-like molecules tends to become small, which should result in the weak correlations between LSI and the other indices. Analyses based on LSI and C-LSI, however, revealed that the switching phenomenon between the structured and destructured states is a most fundamental feature of fluctuations even at temperatures well above the melting point. Other local quantities only have weak correlations to the structure switching fluctuation in such high temperature. Thus, LSI and C-LSI should serve as the fundamental indices to investigate the fluctuations over the wide region of temperature and pressure.

VI. SUMMARY AND DISCUSSION

Through the analyses of the MD data on the local radial distribution of molecules, it was shown that each molecule alternately goes through the structured period and the destructured period. During the structured period water molecule has locally more ordered tetrahedral structure than the average. The order parameter of this structural switching was introduced by using a new method of coarse-graining, and was termed C-LSI. By using this order parameter, it was shown that the structured and destructured molecules have spatial correlations to form the clusters of the structured molecules and the clusters of the destructured molecules. The analysis of the neutron-weighted pair correlation function

showed that the structured molecule is LDA-like and the destructured molecule is HDA-like, so that liquid water is a composite of the LDA-like clusters and the HDA-like clusters even at temperatures well above the melting point. By lowering temperature, the size of the LDA-like clusters grows large and the spatial correlation of the HDA-like molecules becomes stronger. By extrapolating this tendency to the supercooled region, it was expected that at the low enough temperature, under the ambient pressure, the competition between the LDA-like clusters and the HDA-like clusters becomes so large that the system should not settle to be LDA-like or HDA-like as a whole. Further systematic analyses in the lower temperature region are needed to understand whether the hypothesis of the critical point should hold true or not.

LSI and C-LSI were compared with the other local quantities such as the potential energy, the local number of neighboring molecules, the local number of hydrogen bonds, and the local number of rings in the hydrogen-bond network. These quantities, however, describe the structure switching fluctuation not so well as LSI and C-LSI can do. One of the reasons for this imperfect correspondence is because the thermal randomization brings about the variety of different local molecular environment even among the LDA-like molecules or among the HDA-like molecules. Due to the imperfect correspondence between the number of hydrogen bonds and LSI, the four-bonded patches^{14,15} and the LDA-like clusters do not significantly overlap each other.¹⁷

An important question is whether there is a direct experimental means of measuring the LSI or C-LSI fluctuation. In the present study we observed that the characteristic length and lifetime of the structure switching fluctuations distribute from a few Å to at least 10 Å and from several hundred fs to 10 ps at around the melting temperature. For such space and time scales, the dynamical structure factor, $S(q, \omega)$ measured with the quasi-elastic neutron scattering experiment might be an important source of information. Especially, the deviation of the scattering intensity from the one expected from the jump-diffusion model²² should be carefully analyzed. Another possible way to measure the LSI fluctuation is to examine the Raman spectrum. It was shown that the peak around 160 cm^{-1} corresponds to the longitudinal vibration mode, the component around $40\text{--}50 \text{ cm}^{-1}$ corresponds to the transverse vibration mode, and the component around $60\text{--}70 \text{ cm}^{-1}$ is due to the bifurcated hydrogen bond.¹¹ It should be plausible that the longitudinal and transverse vibrations localized around the structured molecules make the larger contribution to the Raman spectrum than the vibrations around the destructured molecules do. The $60\text{--}70 \text{ cm}^{-1}$ component might arise from the localized vibrations around the destructured molecules. In order to establish these relations between the structural switching and the Raman spectrum, more detailed analyses on the vibrational modes are necessary: The Raman intensity can be calculated from the autocorrelation function of the quadratic moment of each molecule. To calculate such quantity with the MD simulation, however, the long range Coulomb interaction should be treated more carefully than in the present paper.²³

Growth and collapse of the LDA-like clusters and the HDA-like clusters should decisively affect the nature of the fluctuations in liquid water. Since water molecules are embedded in the random and percolated network of hydrogen bond, each molecule does not move independently but should move collectively associated with the topological rearrangement of the hydrogen-bond network.²⁴ Such collective motions have to manifest those features in the dynamics of the LDA-like clusters and the HDA-like clusters. The hierarchical distribution of the size of the LDA-like clusters shown in Fig. 8 might be the origin of the fractal nature of the energy fluctuation observed as the $1/f$ -noise over the three decades of the frequency range.²⁵

The molecular scale separation of the system into the LDA-like and HDA-like clusters over the wide temperature region is consistent with the picture that the LDL–HDL transition is responsible for the large fluctuations. Thus the fluctuations found in liquid water at biological temperatures should be regarded as the molecular-scale precursor of the LDL–HDL transition in the supercooled region.

Not only the collective motions in pure water but the hydration dynamics in water solutions should be profoundly affected by this molecular-scale fluctuation. Therefore, further studies on the structure fluctuation may lead to the possibility that the hydration of biomolecules, for example, is described in the language of the phase transition and the critical phenomenon. Analyses of the LSI and C-LSI fluctuations around the solute molecules should open an avenue to the new view of the hydration mechanism.

ACKNOWLEDGMENTS

A part of this work was done while one of the authors (M.S.) was staying at Boston University. M.S. thanks Professor H. Eugene Stanley for the warm hospitality and enlightening discussions during his stay at Boston University. This work was partially supported by the Grant-in-Aid in the Primary Research Area of Protein Architecture and Grant-in-Aid for Scientific Research (No. 09440147) from Ministry of Education, Science, and Culture, Japan.

APPENDIX

In this Appendix we explain the method to erase the fast oscillation components from the MD data. First, a model is developed which can explain the distribution function of LSI. Then, the parameters of the model are tuned to fit the MD data by using the maximum likelihood estimation.¹⁸ The coarse-grained LSI is derived from the parameters obtained in this way.

Distributions of the value of LSI at different temperatures are shown in Fig. (17). Here the distribution of LSI, $P(I)$, is defined as

$$P(I)\Delta I = \frac{1}{N} \langle \Delta n(I, t) \rangle, \quad (\text{A1})$$

where $N=216$ is the total number of molecules, $\Delta n(I, t)$ is the number of molecules whose LSI is within the range $I - \Delta I/2 < I(\mu, t) < I + \Delta I/2$, and $\langle \dots \rangle$ is the average over the MD trajectory. A notable feature of Fig. 17 is that all the

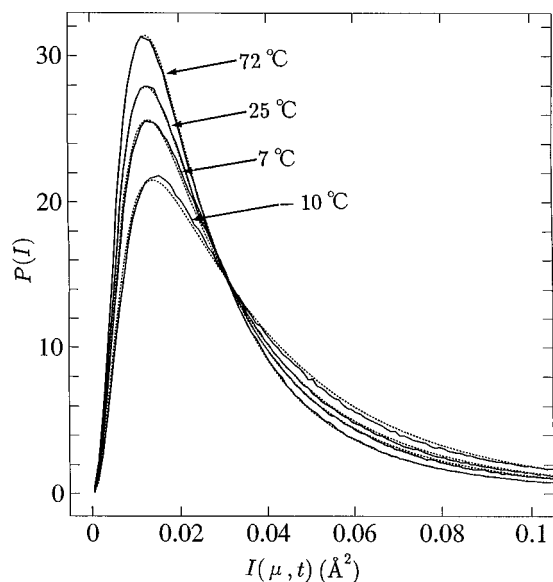


FIG. 17. The distribution of LSI, $P(I)$, at various temperatures under the ambient pressure. Taken from Fig. 5(a) in Ref. 17. The real lines are the MD data and the dashed lines are from Eq. (A2).

curves cross each other at almost the single point of $I \approx 0.03 \text{ \AA}^2$. Therefore, the MD data of $P(I)$ in Fig. 17 can be fitted by superposing two functions, $P_s(I)$ and $P_d(I)$

$$P(I) \cong n_s P_s(I) + (1 - n_s) P_d(I), \quad (\text{A2})$$

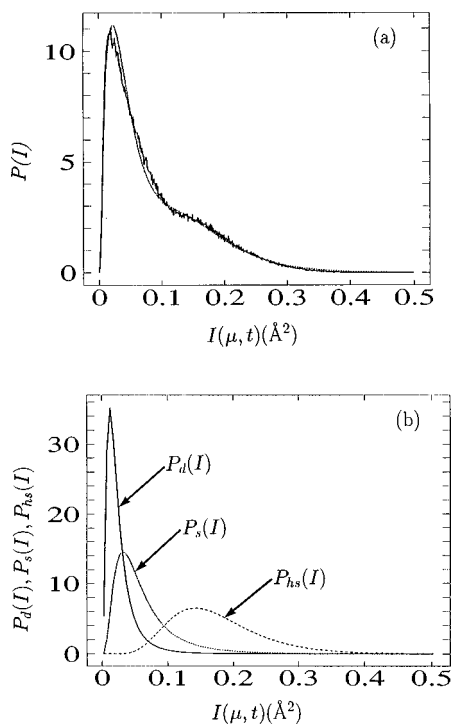


FIG. 18. (a) The distribution of LSI, $P(I)$, at $T = -30^\circ\text{C}$ under the ambient pressure. The real line is the MD data and the dashed line is Eq. (A4). (b) The functional form of the intrinsic distribution of LSI of the destructured molecules $P_d(I)$, the intrinsic distribution of LSI of the moderately structured molecules $P_s(I)$, and the intrinsic distribution of LSI of the highly structured molecules $P_{hs}(I)$.

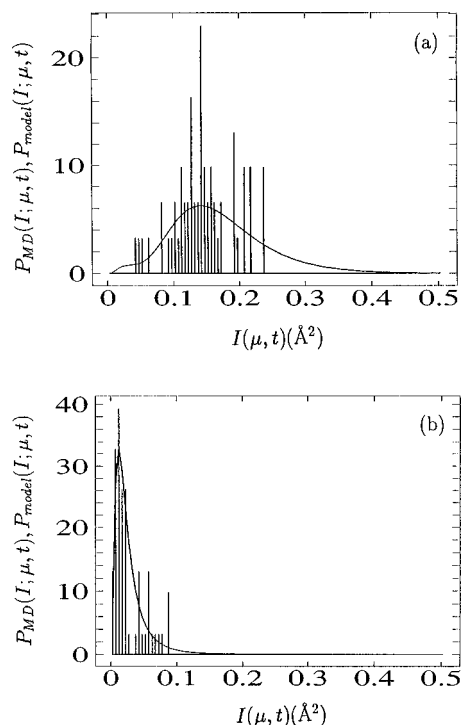


FIG. 19. Distribution of LSI $P_{MD}(I; \mu, t)$ of the arbitrarily chosen molecule μ for the time duration between $t - 300$ fs and $t + 300$ fs is fitted by the model distribution $P_{model}(I; \mu, t)$. $P_{MD}(I; \mu, t)$ is represented by the histogram with the sampling width $\Delta I = 0.005 \text{ \AA}^2$ and $P_{model}(I; \mu, t)$ is a smooth real line. (a) An example that the molecule μ is in the structured state and (b) an example that the molecule μ is in the destructured state. $T = 25^\circ\text{C}$ under the ambient pressure.

where n_s is the weight of superposition and $0 < n_s < 1$. We found that the F -distribution function¹⁸ of the following form can be used as a good approximate representation of $P_s(I)$ or $P_d(I)$:

$$P_s(I) \text{ or } P_d(I) = \frac{\Gamma((m+n)/2)}{\Gamma(m/2)\Gamma(n/2)} \times \alpha m^{m/2} n^{n/2} \frac{(\alpha I)^{m/2-1}}{(m\alpha I + n)^{(m+n/2)}}. \quad (\text{A3})$$

The parameters m , n , and α were optimized so as to fit Eq. (A2) to the MD data: $m = 9$, $n = 9$, and $\alpha = 20$ for $P_s(I)$ and $m = 8$, $n = 8$, and $\alpha = 50$ for $P_d(I)$. $P_s(I)$ and $P_d(I)$ thus obtained are shown in Fig. 18(b). A possible interpretation of Eq. (A2) is that the LSI distribution of the structured molecules is described by $P_s(I)$ and the LSI distribution of the destructured molecule is described by $P_d(I)$. Then, the different value of n_s at different temperature should be due to the different populations of the structured and destructured molecules. Thus, $P_s(I)$ is termed the intrinsic distribution function of LSI of the structured molecules and $P_d(I)$ is termed the intrinsic distribution function of LSI of the destructured molecules.¹⁷ By lowering temperature, however, $P(I)$ begins to cross at different points from $I \approx 0.03 \text{ \AA}^2$. As shown in Fig. 18(a), $P(I)$ at the lower temperature can be fitted again by introducing the third function, $P_{hs}(I)$, the intrinsic distribution function of the highly structured molecules:

$$P(I) \doteq n_{\text{hs}} P_{\text{hs}}(I) + n_s P_s(I) + (1 - n_{\text{hs}} - n_s) P_d(I), \quad (\text{A4})$$

with $0 < n_{\text{hs}} + n_s < 1$ and $0 < n_{\text{hs}} < 1$. $P_{\text{hs}}(I)$ has the same functional form as in Eq. (A3) with the parameters optimized to be $m = 19$, $n = 40$, and $\alpha = 6$.

Based on the interpretation that the LSI distribution of the structured molecules is described by $P_s(I)$ and $P_{\text{hs}}(I)$ and the LSI distribution of the destructured molecule is described by $P_d(I)$, we assume that the equation similar to Eq. (A4) can be used to describe the probabilistic behavior of each molecule during the short period. Validity of this assumption is supported by the results that the probability distribution constructed based on this idea can excellently fit the MD data. We define the probability weight $n_{\text{hs}}(\mu, t)$ that the molecule μ is highly structured at time t , and the probability weight $n_s(\mu, t)$ that the molecule μ is moderately structured at time t . The model probability distribution function $P_{\text{model}}(I; \mu, t)$ is constructed by using the same $P_s(I)$, $P_d(I)$, and $P_{\text{hs}}(I)$ as in Eq. (A4)

$$P_{\text{model}}(I; \mu, t) = n_{\text{hs}}(\mu, t) P_{\text{hs}}(I) + n_s(\mu, t) P_s(I) + (1 - n_{\text{hs}}(\mu, t) - n_s(\mu, t)) P_d(I). \quad (\text{A5})$$

From the MD data, the distribution function $P_{\text{MD}}(I; \mu, t)$ of LSI of the molecule μ during the period from $t - \Delta t/2$ to $t + \Delta t/2$ is given by

$$P_{\text{MD}}(I; \mu, t) \Delta I = \langle \Delta n(I(\mu, t), t) \rangle_{\Delta t}, \quad (\text{A6})$$

where $\Delta n(I(\mu, t), t) = 1$ when the observed LSI value of the molecule μ is within the range $I - \Delta I/2 < I(\mu, t) < I + \Delta I/2$ at time t , and $\Delta n(I(\mu, t), t) = 0$ otherwise. $\langle \dots \rangle_{\Delta t}$ is the average over the period from $t - \Delta t/2$ to $t + \Delta t/2$. We used $\Delta t = 600$ fs and $\Delta I = 0.005 \text{ \AA}^2$. The weights $n_{\text{hs}}(\mu, t)$ and $n_s(\mu, t)$ in Eq. (A5) are determined, so that $P_{\text{model}}(I; \mu, t)$ becomes the best model of $P_{\text{MD}}(I; \mu, t)$. In order to find the best model, the likelihood function $L(n_{\text{hs}}(\mu, t), n_s(\mu, t))$ is defined by

$$L(n_{\text{hs}}(\mu, t), n_s(\mu, t)) = \left\langle \sum_{I(\mu, t)} \log(P_{\text{model}}(I; \mu, t)) \Delta n(I(\mu, t), t) \right\rangle_{\Delta t}. \quad (\text{A7})$$

Then, $n_{\text{hs}}(\mu, t)$ and $n_s(\mu, t)$ are determined so as to maximize $L(n_{\text{hs}}(\mu, t), n_s(\mu, t))$. The optimized $P_{\text{model}}(I; \mu, t)$ can excellently fit $P_{\text{MD}}(I; \mu, t)$, which supports the assumptions we made to derive Eq. (A5). Figures 19(a) and 19(b) are examples of the fitting. Therefore, $n_{\text{hs}}(\mu, t)$ and $n_s(\mu, t)$ obtained in this way can be used as measures how the molecule is structured. We define

$$A(\mu, t) = n_{\text{hs}}(\mu, t) + n_s(\mu, t), \quad (\text{A8})$$

as a new index of the local structure and call $A(\mu, t)$ the coarse-grained LSI (C-LSI). We believe the method developed here is not restricted to the LSI analysis but is also applicable to other problems in the liquid state.

- ¹For reviews, see P. G. Debenedetti, *Metastable Liquids* (Princeton University Press, Princeton, New Jersey 1997); C. A. Angell, *Science* **267**, 1924 (1995).
- ²R. J. Speedy, *Nature (London)* **380**, 289 (1996).
- ³S. Sastry, P. G. Debenedetti, F. Sciortino, and H. E. Stanley, *Phys. Rev. E* **53**, 6144 (1996).
- ⁴O. Mishima, L. D. Calvert, and E. Whalley, *Nature (London)* **314**, 76 (1985).
- ⁵O. Mishima, *J. Chem. Phys.* **100**, 5910 (1994).
- ⁶P. H. Poole, F. Sciortino, T. Grande, H. E. Stanley, and C. A. Angell, *Phys. Rev. Lett.* **73**, 1632 (1994).
- ⁷P. H. Poole, F. Sciortino, U. Essmann, and H. E. Stanley, *Nature (London)* **360**, 324 (1992).
- ⁸H. E. Stanley, L. Cruz, S. T. Harrington, P. H. Poole, S. Sastry, F. Sciortino, F. W. Starr, and R. Zhang, *Physica A* **236**, 19 (1997).
- ⁹S. Harrington, R. Zhang, P. H. Poole, F. Sciortino, and H. E. Stanley, *Phys. Rev. Lett.* **78**, 2409 (1997).
- ¹⁰H. Tanaka, *Nature (London)* **380**, 328 (1996); *J. Chem. Phys.* **105**, 5099 (1996).
- ¹¹Y. C. Chu and G. E. Walrafen, in *Hydrogen Bond Networks*, edited by M.-C. Bellissent-Funnel and J. C. Dore (Kluwer, Dordrecht, 1994), p. 169; G. E. Walrafen, M. R. Fisher, M. S. Hokmabadi, and W.-H. Yang, *J. Chem. Phys.* **85**, 6970 (1986).
- ¹²G. E. Walrafen, M. S. Hokmabadi, and W.-H. Yang, *J. Chem. Phys.* **85**, 6964 (1986).
- ¹³J.-P. Shih, S.-Y. Sheu, and C.-Y. Mou, *J. Chem. Phys.* **100**, 2202 (1994).
- ¹⁴H. E. Stanley and J. Teixeira, *J. Chem. Phys.* **73**, 3404 (1980).
- ¹⁵H. E. Stanley, R. L. Blumberg, and A. Geiger, *Phys. Rev. B* **28**, 1626 (1983).
- ¹⁶W. L. Jorgensen, J. Chandrasekhar, J. D. Madura, R. W. Impey, and M. L. Klein, *J. Chem. Phys.* **79**, 926 (1983).
- ¹⁷E. Shiratani and M. Sasai, *J. Chem. Phys.* **104**, 7671 (1996).
- ¹⁸For a text book, B. W. Lindgren, *Statistical Theory* (Macmillan, New York, 1976).
- ¹⁹M. R. Chowdhury, J. C. Dore, and J. T. Wenzel, *J. Non-Cryst. Solids* **53**, 247 (1982).
- ²⁰M.-C. Bellissent-Funnel, J. Teixeira, and L. Bosio, *J. Chem. Phys.* **87**, 2231 (1987).
- ²¹G. Rucco, M. Sampoli, A. Torcini, and R. Vallauri, *J. Chem. Phys.* **99**, 8095 (1993).
- ²²P. A. Egelstaff, *An Introduction to the Liquid State* (Academic, London, 1967).
- ²³S. Saito and I. Ohmine, *J. Chem. Phys.* **102**, 3566 (1995).
- ²⁴I. Ohmine and H. Tanaka, *Chem. Rev.* **93**, 2545 (1993).
- ²⁵M. Sasai, I. Ohmine, and R. Ramaswamy, *J. Chem. Phys.* **96**, 3045 (1992).
- ²⁶E. Whalley, D. D. Klug, and Y. P. Handa, *Nature (London)* **342**, 782 (1989).